RESEARCH ARTICLE

morphology WILEY

Comparative morphological examination of vertebral bodies of teleost fish using high-resolution micro-CT scans

Misaki Sakashita[1] 🆔 | Mao Sato[2] 🆔 | Shigeru Kondo[1]

[1]Graduate School of Frontier Biosciences, Osaka University, Osaka, Japan

[2]Laboratory of Marine Biology, Faculty of Science, Kochi University, Kochi, Japan

Correspondence
Misaki Sakashita, Graduate School of Frontier Biosciences, Osaka University, 1-3 Yamadaoka, Suita, Osaka, Japan 565-0871.
Email: sakashitamsk@gmail.com

Abstract

Vertebral bodies of teleost fish are formed by the sclerotomal bone covering the chordacentrum. The internal part of the sclerotomal bone is composed of an amphicoelous hourglass shaped autocentrum, which is common in most fish species. In contrast, the external shape of the sclerotomal bone varies extensively among species. There are multiple hypotheses regarding the composition and formation of the external structure. However, as they are based on studies of few extant or extinct species, their applicability to other species remains to be clarified. To understand the morphology, formation, and composition of vertebral bodies in teleosts, we performed a comparative analysis using micro-CT scans of 32 species from 10 orders of Teleostei and investigated the detailed morphology of the sclerotomal bone, especially its plate-like ridge and trabeculae. We discovered two structural characteristics that are shared among most of the examined species. One was the sheet-like trabeculae that extend radially from the center of the vertebral body with a constant thickness. The other was the presence of hollow spaces on the internal parts of the lateral ridge and trabeculae. The combination of different arrangements of sheet-like trabeculae and internal hollow spaces formed different shapes of the lateral structure of the vertebral body. The properties of these two characteristics suggest that the external part of the sclerotomal bone grows outward by deposition at the bone tip, and that, concurrently, bone absorption occurs in the internal part of the sclerotomal bone. The vertebral arches were also formed by the sheet-like trabeculae, indicating that both, the vertebral body and the arches, are formed by the same component. The micro-CT scanning data were uploaded to a public database so they can be used for future studies on fish vertebrae.

KEYWORDS
arcocentrum, autocentrum, development, trabecula

1 | INTRODUCTION

The vertebral column is an essential structure that supports the body of vertebrates on an axis. As the vertebral column is formed by several linearly connected vertebrae, its support physically depends on vertebral morphology. For this reason, the morphology of the vertebral body and its formation has been an important theme of anatomical studies. Teleost fish represent the most speciose group among vertebrates (Betancur-R et al., 2013; Near et al., 2012; Nelson, Grande, & Wilson, 2016), and the shapes of vertebrae vary among species (Arratia, 1991; Arratia, Schultze, & Casciotta, 2001). In the last 20 years, intensive research has been conducted on zebrafish, *Danio*

rerio (Hamilton) and on the Atlantic salmons, *Salmo salar* Linnaeus using histological or molecular biology methods (Fleming, Kishida, Kimmel, & Keynes, 2015), and many aspects of morphology and developmental processes of fish vertebral bodies have been revealed.

The first step in the development of vertebral bodies is mineralization, which occurs within the notochordal sheath and forms the cylindrical chordacentrum (Bensimon-Brito, Cardeira, Cancela, Huysseune, & Witten, 2012; Grotmol, Kryvi, Nordvik, & Totland, 2003; Inohaya, Takano, & Kudo, 2007). Chordoblasts or osteoblasts derived from sclerotomes are responsible for this mineralization (Bensimon-Brito et al., 2012; Grotmol et al., 2003; Inohaya et al., 2007; Willems et al., 2012). The spatial pattern of the chordacentrum is determined by the segmental pattern of the notochord (Bensimon-Brito et al., 2012; Fleming, Keynes, & Tannahill, 2004; Grotmol, Nordvik, Kryvi, & Totland, 2005; Wopat et al., 2018). After the formation of the chordacentrum, osteoblasts derived from sclerotomes deposit bone matrix on the external surface of the chordacentrum. The resulting bone is called sclerotomal bone (Grotmol et al., 2003). Because the sclerotomal bone continues to grow outward, most of the vertebral body of an adult fish is formed by sclerotomal bone. Many studies have proposed different interpretations and nomenclatures for the parts composing the sclerotomal bone. However, according to the study on the Atlantic salmon by Nordvik, Kryvi, Totland, and Grotmol (2005), the sclerotomal bone is divided into two different parts: internally, the bone is dense and formed by the ossification of the parallel-oriented collagen matrix, whereas, externally, the bone is less dense and formed by the ossification of the woven collagen matrix. The internal and external parts of the bone constitute the autocentrum and the arcocentrum, respectively (Nordvik et al., 2005). The autocentrum has an amphicoelous hourglass shape, formed by a continuous addition of bone matrix at the edge of the hourglass-shaped structure (Inohaya et al., 2007; Nordvik et al., 2005). This hourglass shape has been widely observed in actinopterygians, and its morphology among the group is invariable (Arratia et al., 2001; Laerm, 1976). Therefore, the developmental process of the hourglass-shaped structure may be common among actinopterygians.

However, the shape of the arcocentrum that composes the lateral structure of the vertebral body varies substantially among teleosts and exhibits various morphologies with different arrangements of foramina, grooves, and crests (Arratia, 1991; Eastman, Witmer, Ridgely, & Kuhn, 2014; Laerm, 1976; Nordvik et al., 2005). Nordvik et al. (2005) found that osteoblasts were located only on the external surface of the arcocentrum in the Atlantic salmon, suggesting that the growth of the arcocentrum also occurred by the deposition of the bone material to its end (Nordvik et al., 2005). However, as the shape of lateral structures differs among species, it is unclear whether findings in Atlantic salmons are applicable to other species. Detailed comparative studies based on a broader range of species are needed to reach a general understanding of the anatomy of vertebral bodies in teleosts. The analysis and comparison, not only of external shape among species, but also of internal microstructure, would allow an estimation of the basic vertebral body structure among teleost species and the causes of external shape variation. In this context, we collected vertebral bodies of 32 species from 10 orders of Teleostei and performed high-resolution micro-CT scans on them. Based on the analysis of the obtained 3D data, we described characteristics of macroscopic shapes in each species and investigated the detailed structural features shared by the species. Based on these features, we propose a formation process of vertebral lateral structure.

2 | MATERIALS & METHODS

2.1 | Fish specimens

To perform a comparative morphological study including a wide range of phylogenetic groups, we collected 51 individuals of 32 species from 10 orders of Teleostei (Table 1). All individuals were obtained by commercial bottom trawling at the coast of the Japan archipelago, or purchased on fish markets in Japan, between 2016 and 2018. Detailed collection locations of each specimen are in Table 1. Fish identification followed Nakabo (2013). We measured the standard body length (SL) of each specimen; total length (TL) is provided when SL could not be determined. When neither SL nor TL could not be determined, we calculated the sum of lengths of all vertebrae, except the urostyle. Body lengths varied from 14 to 107% of the approximate maximum known SL or TL described for each species in Masuda et al. (1984) and Nakabo (2013); Table 1). As per the definition of Kendall Jr., Ahlstrom, and Moser (1984), all specimens examined were past the juvenile stage. All specimens were considered to be adults or in immature adult stages, although we did not examine gonad maturity. Specimens with body length over 50% of the approximate maximum known body SL or TL (following Masuda et al., 1984 and Nakabo, 2013) were considered to be adults.

2.2 | Preparation of skeletal specimens

To prepare the skeletal specimens, we first boiled the fish for approximately 15 to 30 min, depending on the size of fish, until the body tissues were completely heated. Then, we roughly removed the muscles and the bones were cleaned by immersion in trypsin solution (trypsin [BECTON DICKINSON Difco Trypsin 250] 1 g in milliQ) for 1 day at 37 °C or in 2% NaOH solution (sodium hydroxide [Wako] 20 mg/mL in milliQ) for approximately 3 h at room temperature (24–25 °C; see immersion solution in Table 1). We then removed the remaining tissues using running water and air-dried the bones at room temperature (24–25 °C). We observed the vertebrae in lateral view using a Leica MZ-16FA fluorescence stereomicroscope (Leica Microsystems, Wetzlar, Germany).

2.3 | Micro-CT scanning

In most fish species, the shape of the vertebral body varies depending on the anatomical position of the spinal column. In particular, the differences in the shape of the distal vertebral bodies are large; therefore, they are not suitable for comparisons among species. Conversely, the shape of the vertebral bodies at the midpoint of the

TABLE 1 Data for the 51 specimens of 32 species of Teleostei examined with micro-CT scans

Species	N	Location	Anatomical position	Standard length (mm)	Maximum known SL or TL (mm)	Body length ratio	Immersed solution
Anguilliformes							
Muraenesox cinereus (Forsskål)	1	Harimanada, Hyogo prefecture	65	860*	2200*	0.39	Trypsin
Clupeiformes							
Sardinops melanostictus (Temminck & Schlegel)	3	The Pacific coast of Kinki district	16/16/16	185/198/198	240	0.77	Trypsin
Konosirus punctatus (Temminck & Schlegel)	4	The Pacific coast of Kinki district	8/16/16/12	127/130/131/135	260	0.49	Trypsin
Osmeriformes							
Plecoglossus altivelis altivelis (Temminck & Schlegel)	1	The Pacific coast of Kinki district	34	227	300	0.76	Trypsin
Lophiiformes							
Lophiomus setigerus (Vahl)	1	The Pacific coast of Kochi prefecture	7	285	1,000	0.29	Trypsin
Lophius litulon (Jordan)	1	Hakodate, Hokkaido prefecture	7	452	1,500	0.30	NaOH
L. litulon	1	Sakaiminato, Tottori prefecture	8	623	1,500	0.42	Trypsin
Chaunax abei Le Danois	3	Mimase, Kochi prefecture	5/4/4	178/188/209	300	0.59	Trypsin
Zeiformes							
Zenopsis nebulosa (Temminck & Schlegel)	1	The Pacific coast of Kochi prefecture	8	360	500	0.72	Trypsin
Zeus faber Linnaeus	3	The Pacific coast of Kochi prefecture	6/6/7	210*/300*/359	300	0.70	NaOH
Gasterosteiformes							
Macroramphosus sagifue Jordan & Starks	2	Mimase, Kochi prefecture	9/9	89/90	170	0.52	Trypsin
Beloniformes							
Cololabis saira (Brevoort)	2	The Pacific coast of Kinki district	40/40	274/281	350	0.78	Trypsin
Perciformes							
Helicolenus hilgendorfii (Döderlein)	2	The Pacific coast of Kochi prefecture	6/6	145/177	270	0.54	Trypsin
Sebastes oblongus Günther	1	Noto peninsula, Ishikawa prefecture	7	240*	350	0.69	NaOH
Sebastes zonatus Chen & Barsukov	1	Noto peninsula, Ishikawa prefecture	11	120**	370	0.32	NaOH
Chelidonichthys spinosus (McClelland)	2	The Pacific coast of Kochi prefecture	10/11	223/237	400*	0.56	Trypsin
Acropoma hanedai Matsubara	1	Mimase, Kochi prefecture	8	82	110	0.75	Trypsin
Trachurus japonicus (Temminck & Schlegel)	1	Noto peninsula, Ishikawa prefecture	8	320*	300	1.07	NaOH
Pagrus major (Temminck & Schlegel)	1	Noto peninsula, Ishikawa prefecture	8	230*	1,000	0.23	NaOH

(Continues)

TABLE 1 (Continued)

Species	N	Location	Anatomical position	Standard length (mm)	Maximum known SL or TL (mm)	Body length ratio	Immersed solution
Sillago japonica Temminck & Schlegel	2	The coast of the sea of Japan, Tottori prefecture	15/15	188/211	300	0.63	Trypsin
Histiopterus typus Temminck & Schlegel	1	The Pacific coast of Kochi prefecture	10	80	350	0.23	Trypsin
Scarus forsteni (Bleeker)	1	Okinawa prefecture	9	182	400	0.46	Trypsin
Sphyraena pinguis Günther	2	The Pacific coast of Kochi prefecture	12/12	264/291	300	0.88	Trypsin
Rexea prometheoides (Bleeker)	1	The Pacific coast of Kochi prefecture	10	278	400	0.70	Trypsin
Scomber japonicus Houttuyn	1	The Pacific coast of Chiba prefecture	11	298	500	0.60	Trypsin
Thunnus orientalis (Temminck & Schlegel)	1	Hamasaka, Shizuoka prefecture	10	429	3,000	0.14	Trypsin
T. orientalis	1	The coast of the sea of Japan, Tottori prefecture	10	558	3,000	0.19	NaOH
Thunnus tonggol (Bleeker)	1	The Pacific coast of Kinki district	9	550*	1,000	0.55	NaOH
Pleuronectiformes							
Paralichthys olivaceus (Temminck & Schlegel)	1	Noto peninsula, Ishikawa prefecture	7	218	850	0.26	Trypsin
Hippoglossoides dubius Schmidt	1	Noto peninsula, Ishikawa prefecture	14	150**	450	0.33	NaOH
Tetraodontiformes							
Macrorhamphosodes uradoi (Kamohara)	3	Mimase, Kochi prefecture	6/6/5	93/126/146	150	0.62	Trypsin
Takifugu pardalis (Temminck & Schlegel)	1	The Pacific coast of Mie prefecture	7	170*	300	0.57	NaOH
Takifugu snyderi (Abe)	1	The Pacific coast of Mie prefecture	4	210*	300	0.70	NaOH
Takifugu stictonotus (Temminck & Schlegel)	1	The Pacific coast of Kinki district	8	93**	350	0.27	NaOH

Notes. Location indicates where in Japan the individual was caught. Individuals of the same species that were caught in different locations are described separately. If the number of individuals (N) is more than or equal to 2 (N ≥ 2), all individuals were caught in the same location. Anatomical position indicates the vertebra(e) examined with micro-CT scans. In Standard length (SL), * indicates total length (TL) and ** indicates the sum of the lengths of all vertebrae (SLV), except the urostyle. In Anatomical position and Standard length, the arrangement of values is from the smallest to the largest specimen. Maximum known SL or TL follows Masuda, Amaoka, Araga, Uyeno, and Yoshino (1984), except H. hilgendorfii and S. zonatus; for these two species, we followed Nakabo (2013). Body length ratio indicates the ratio of Standard length of the specimen to the Maximum SL or TL known. If multiple individuals of the same species were examined with CT scans, the value of the smallest specimen is described. Immersed solution indicates the solution in which vertebrae were immersed for flesh digestion.

spinal column, including the first hemal arch, is similar. Therefore, these vertebrae are suitable for a comparative analysis among species. Moreover, the first hemal arch can be easily distinguished from other vertebrae in the same individual. For this reason, the vertebral body with the first hemal arch was chosen to be used in this comparative analysis.

We scanned the skeletal specimens of vertebral bodies from each individual using a micro–CT-scanner SkyScan 1,172 (SkyScan NV, Aartselaar, Belgium) following manufacturer's instructions. For stable positioning, we fixed each specimen to the stage using double-sided tape. The X-ray source ranged from 50–80 kV, and the datasets were acquired at a resolution of 2–14 μm/pixel, depending on the size of each vertebral body. We reconstructed the stacks of transverse sections from primary shadow images using SkyScan software NRecon (Version 1. 7. 1. 0). From these image stacks, we constructed 3D volume-rendered images using SkyScan software CT Vox (Version 3. 3. 0). We uploaded the stacks of tomographic images to Systems Science of Biological Dynamics (SSBD) Database (http://ssbd.qbic. riken.jp/set/20190301/) to make them publicly available.

To confirm whether the procedures to prepare the skeletal specimens (boiling, digesting, and drying) for high-resolution micro-CT images altered the morphology of the vertebrae, we examined the same vertebrae of *Lophius litulon* and *Thunnus orientalis* using micro-CT scans immediately after each procedure. To avoid drying of the specimens, they were wrapped with cellophane during the micro-CT scans. Comparing the micro-CT images of each step of the procedure, we confirmed that these procedures did not change the microstructure of the vertebral body (Figures S1 and S2).

2.4 | Measurement of the sheet-like bone thickness

We measured the thickness of the sheet-like bones using the transverse section at the midpoint of each vertebra with the first hemal arch. To distinguish each sheet-like trabecula clearly, we first generated a binary image of the transverse section by thresholding with a variation of the IsoData algorithm using ImageJ (https://imagej.nih. gov/ij/). Then, we obtained the profile of brightness within the range of 0–255 using the Plot Profile function (Figure S3. 1). We defined a sheet-like trabecula as each rectangular wave of the profile and its thickness as the peak width on the axis where the brightness equals 0 (Figure S3. 2).

3 | RESULTS

Whether the outermost lateral side of vertebral bodies, which was the focus of our study, is formed by arcocentrum or autocentrum in teleosts is still debated. According to Nordvik et al. (2005), in Atlantic salmon the outermost side is formed by arcocentrum, whereas Arratia et al. (2001) stated that in teleosts the entire lateral side consists of autocentrum. Therefore, in this article, we use the term "sclerotomal bone" to indicate the bone that forms on the external side of vertebral bodies and discuss the components of this side.

3.1 | Data of skeletal specimens

Figure 1 shows images obtained using a stereoscopic microscope of the external morphology of the vertebral bodies from 32 species. These images allowed the observation of differences in vertebral body shape, but their resolution was not sufficient to detect differences in the fine structures. Figure 2 shows the volume-rendered micro-CT images in which the fine surface structure was clearly observed. Figure 3 shows images of the transverse sections obtained from the CT-image at the midpoint of each vertebral body, with which the fine surface structure was clearly observed. These images allowed the detection of fine structures that were difficult to identify using conventional microscopic observations.

3.2 | Characteristics of the sclerotomal bone shape in various species

Among the observed species, the internal part of the sclerotomal bone was commonly an hourglass shape as described in previous studies (Laerm, 1976; Arratia et al., 2001. See Figure S4), whereas the external lateral structures exhibited many different shapes (Figure 2). In most species, the lateral structures were composed of the longitudinal trabeculae and ridges (thick trabeculae) running along the craniocaudal direction. Their number, thickness, and angle showed considerable variability among species. We also noted the presence of circular dimples on the surface of vertebral bodies that was commonly found in Perciformes. The morphological characteristics listed below were shared among the multiple individuals we examined from the same species.

3.2.1 | Anguilliformes

In *Muraenesox cinereus* (Daggertooth pike conger), vertebral bodies had multiple branched longitudinal trabeculae, and a single transverse trabecula along the midpoint of the vertebral body (Figure 2[1]).

3.2.2 | Clupeiformes

In *Sardinops melanostictus* (Japanese pilchard), vertebral bodies had a little thick and low longitudinal ridge extending from the base of the neural arch to the lateral side of the vertebral body (Figure 2[2]). In *Konosirus punctatus* (Dotted gizzard shad), vertebral bodies had three longitudinal ridges and two transverse ridges on the lateral side of the vertebral body (Figure 2[3]). All ridges were thin and low.

3.2.3 | Osmeriformes

In *Plecoglossus altivelis altivelis* (Ayu sweetfish), the vertebral body had six longitudinal ridges (Figure 2[4]), between which thin transverse trabeculae were formed.
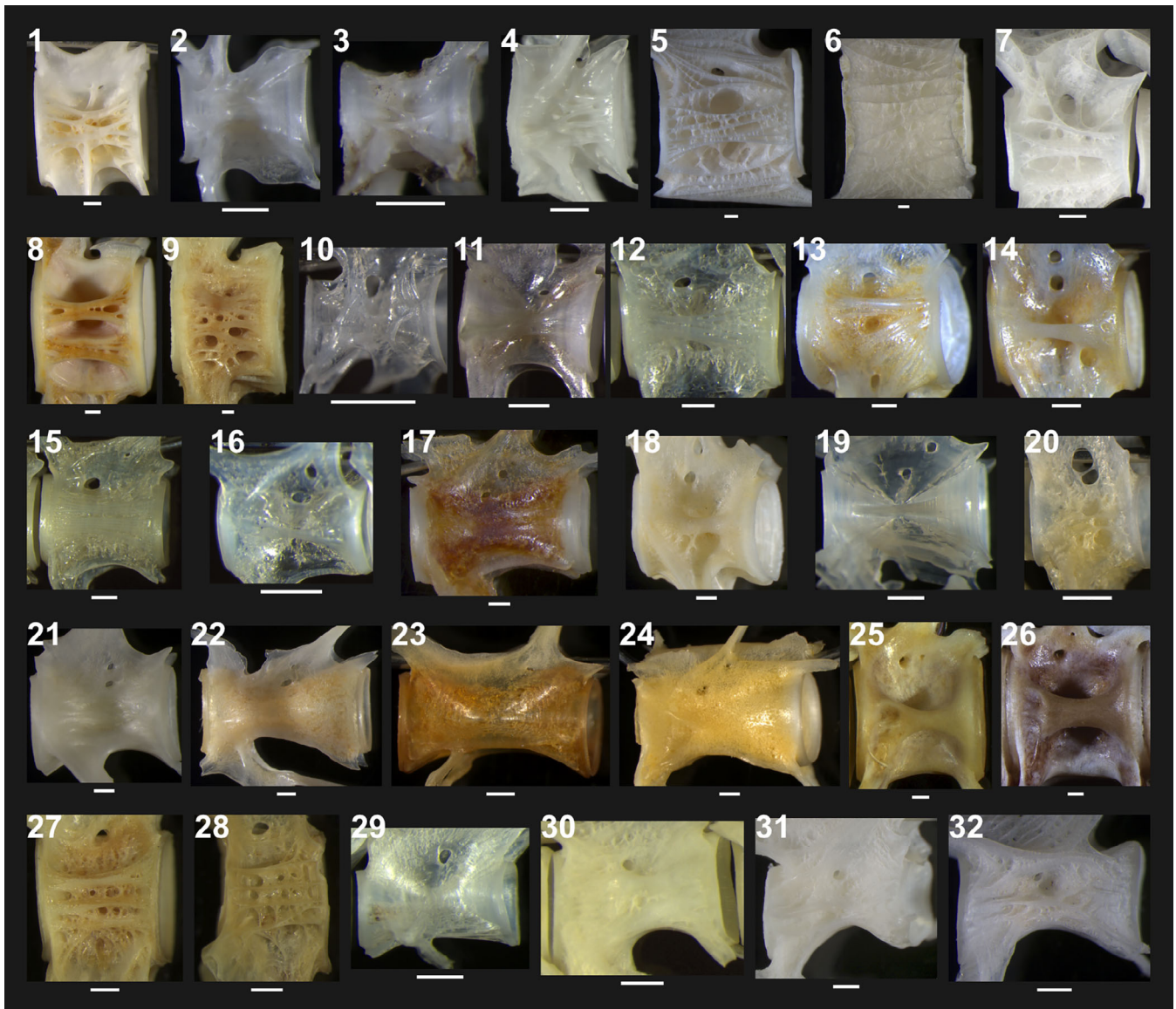
FIGURE 1 Stereoscopic microscope images of the left lateral views of the vertebral bodies with the first hemal arch. (1) *Muraenesox cinereus*, (2) *Sardinops melanostictus* (SL = 185 mm), (3) *Konosirus punctatus* (SL = 135 mm), (4) *Plecoglossus altivelis altivelis*, (5) *Lophiomus setigerus*, (6) *Lophius litulon* (SL = 452 mm), (7) *Chaunax abei* (SL = 188 mm), (8) *Zenopsis nebulosa*, (9) *Zeus faber* (SL = 359 mm), (10) *Macroramphosus sagifue* (SL = 90 mm), (11) *Cololabis saira* (SL = 281 mm), (12) *Helicolenus hilgendorfii* (SL = 177 mm), (13) *Sebastes oblongus*, (14) *Sebastes zonatus*, (15) *Chelidonichthys spinosus* (SL = 237 mm), (16) *Acropoma hanedai*, (17) *Trachurus japonicus*, (18) *Pagrus major*, (19) *Sillago japonica* (SL = 211 mm), (20) *Histiopterus typus*, (21) *Scarus forsteni*, (22) *Sphyraena pinguis* (SL = 291 mm), (23) *Rexea prometheoides*, (24) *Scomber japonicus*, (25) *Thunnus orientalis* (SL = 429 mm), (26) *Thunnus tonggol*, (27) *Paralichthys olivaceus*, (28) *Hippoglossoides dubius*, (29) *Macrorhamphosodes uradoi* (SL = 146 mm), (30) *Takifugu pardalis*, (31) *Takifugu snyderi*, (32) *Takifugu stictonotus*. Yellow or brown parts in the images are the discolored adipose tissues. Scale bars: 1 mm

3.2.4 | Lophiiformes

The vertebral bodies of *Lophiomus setigerus* (Blackmouth angler), *Lophius litulon* (Yellow goosefish), and *Chaunax abei* had a net-like structure formed by many thin sheet-like longitudinal and transverse trabeculae (Figures 2 [5–7]). Transverse trabeculae were between the longitudinal trabeculae. In *Lophiomus setigerus*, many longitudinal trabeculae were on the entire lateral side of the vertebral body and on the neural and hemal arches. Longitudinal trabeculae were particularly concentrated in the mid-lateral side (Figure 2[5]). In *Lophius litulon*, many longitudinal trabeculae were also on

the entire lateral side but more sparsely lined. Also, more transverse trabeculae were between longitudinal trabeculae (Figure 2[6]). Compared to these two species, in *Chaunax abei*, less trabeculae were on the lateral side of the vertebral body. Three longitudinal trabeculae and multiple transverse trabeculae were mainly in the middle of the lateral side (Figure 2[7]).

3.2.5 | Zeiformes

The vertebral bodies of *Zenopsis nebulosa* (Mirror dory) and *Zeus faber* (John dory) had two longitudinal plate-like ridges formed by closely
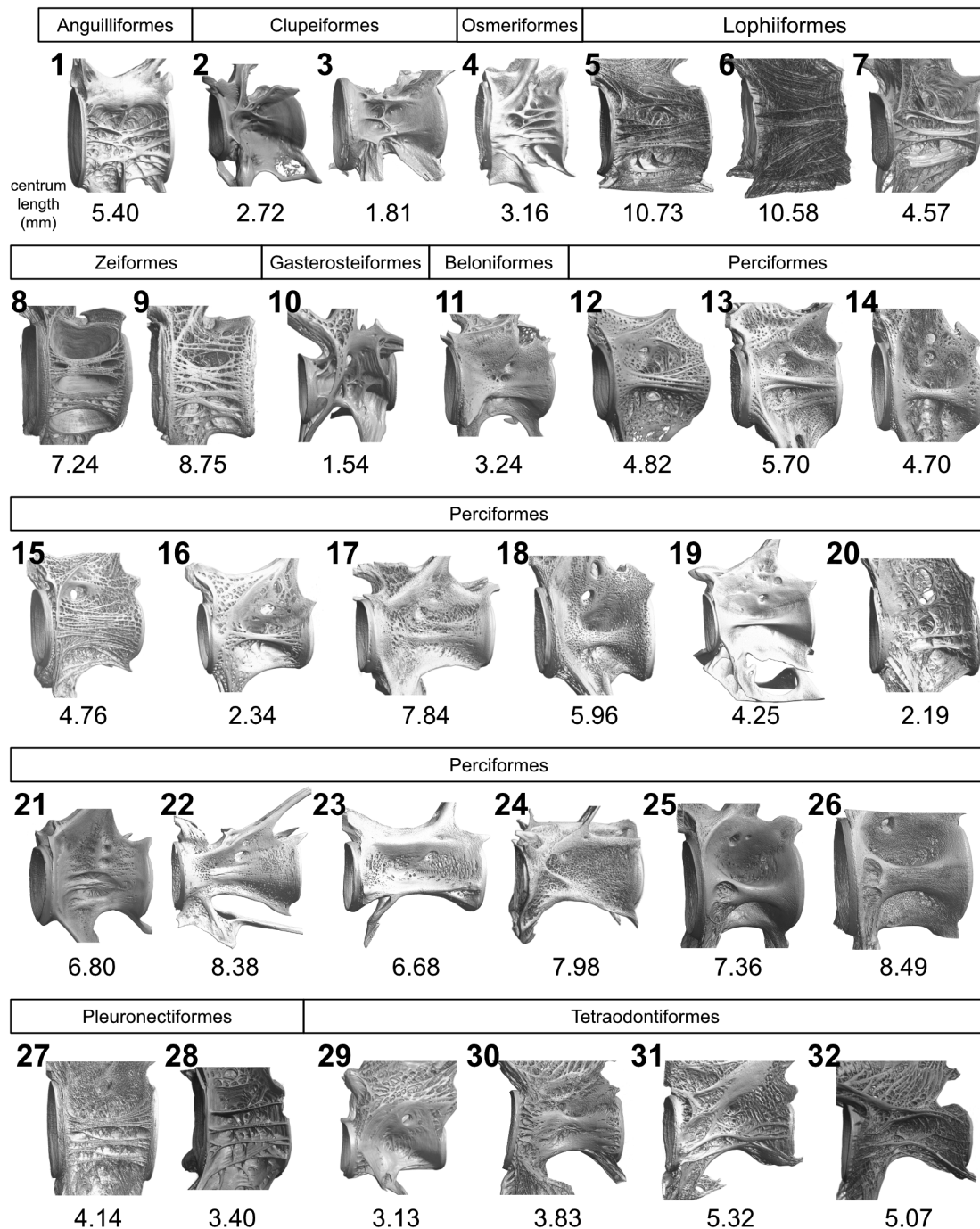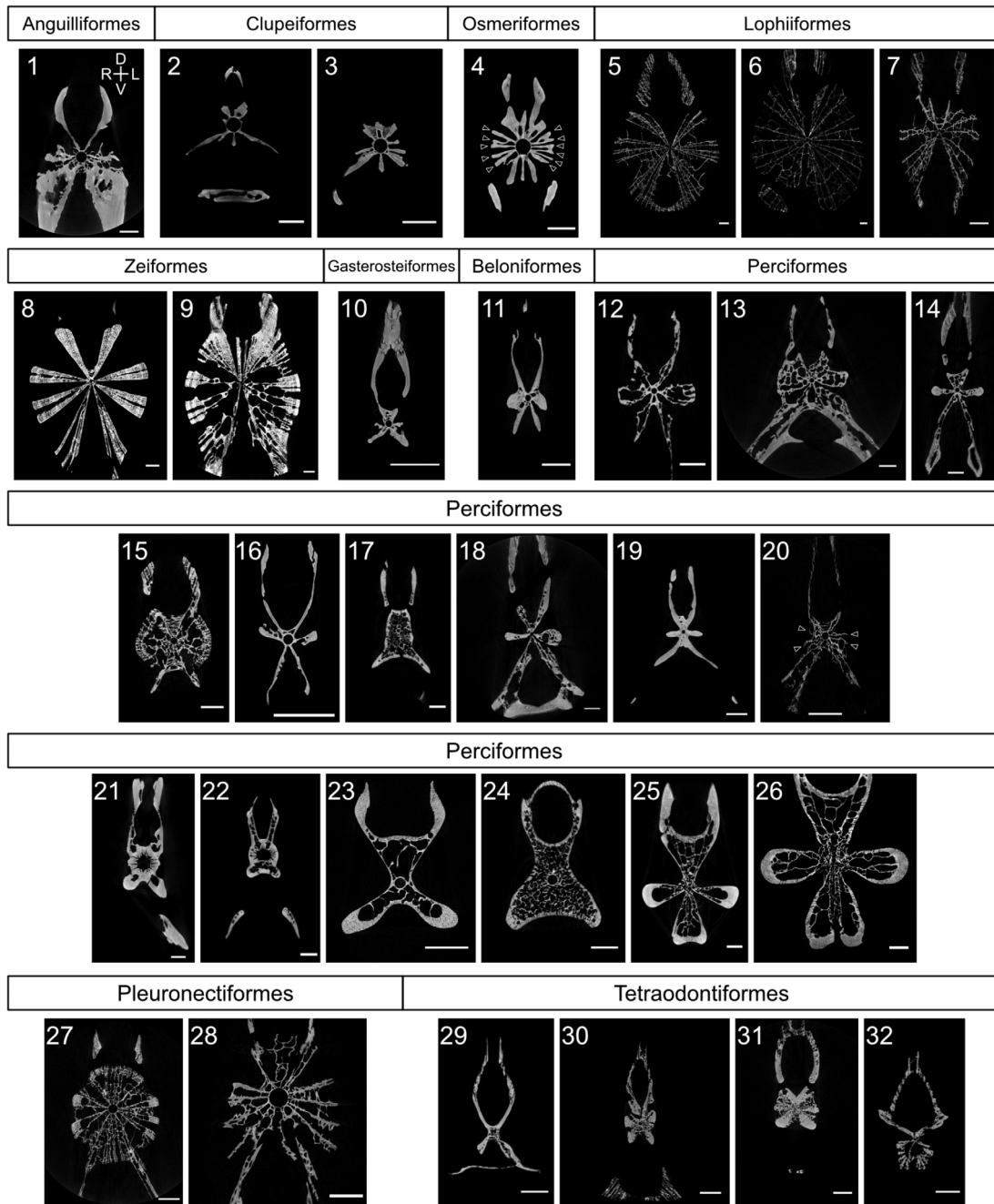
FIGURE 2 Volume-rendered micro-CT images of the left lateral views of the vertebral bodies with the first hemal arch. All vertebral bodies are the same as in Figure 1. (1) *Muraenesox cinereus*, (2) *Sardinops melanostictus* (SL = 185 mm), (3) *Konosirus punctatus* (SL = 135 mm), (4) *Plecoglossus altivelis altivelis*, (5) *Lophiomus setigerus*, (6) *Lophius litulon* (SL = 452 mm), (7) *Chaunax abei* (SL = 188 mm), (8) *Zenopsis nebulosa*, (9) *Zeus faber* (SL = 359 mm), (10) *Macroramphosus sagifue* (SL = 90 mm), (11) *Cololabis saira* (SL = 281 mm), (12) *Helicolenus hilgendorfii* (SL = 177 mm), (13) *Sebastes oblongus*, (14) *Sebastes zonatus*, (15) *Chelidonichthys spinosus* (SL = 237 mm), (16) *Acropoma hanedai*, (17) *Trachurus japonicus*, (18) *Pagrus major*, (19) *Sillago japonica* (SL = 211 mm), (20) *Histiopterus typus*, (21) *Scarus forsteni*, (22) *Sphyraena pinguis* (SL = 291 mm), (23) *Rexea prometheoides*, (24) *Scomber japonicus*, (25) *Thunnus orientalis* (SL = 429 mm), (26) *Thunnus tonggol*, (27) *Paralichthys olivaceus*, (28) *Hippoglossoides dubius*, (29) *Macrorhamphosodes uradoi* (SL = 146 mm), (30) *Takifugu pardalis*, (31) *Takifugu snyderi*, (32) *Takifugu stictonotus*. Lengths of the vertebral centrum in the cranial-caudal direction are displayed below each image

attached multiple longitudinal trabeculae (Figures 2[8, 9]). In *Zenopsis nebulosa*, transverse trabeculae were only on the edge of each ridge (Figure 2[8]), whereas in *Zeus faber*, transverse trabeculae were on the entire lateral side and between the longitudinal trabeculae (Figure 2[9]).

3.2.6 | Gasterosteiformes

In *Macroramphosus sagifue*, vertebral bodies had one longitudinal thin ridge and three transverse ridges on the lateral side

FIGURE 3 Transverse sections at the midpoint of the vertebral bodies with the first hemal arch. All vertebral bodies are the same as in Figure 1. (1) *Muraenesox cinereus*, (2) *Sardinops melanostictus* (SL = 185 mm), (3) *Konosirus punctatus* (SL = 135 mm), (4) *Plecoglossus altivelis altivelis*, (5) *Lophiomus setigerus*, (6) *Lophius litulon* (SL = 452 mm), (7) *Chaunax abei* (SL = 188 mm), (8) *Zenopsis nebulosa*, (9) *Zeus faber* (SL = 359 mm), (10) *Macroramphosus sagifue* (SL = 90 mm), (11) *Cololabis saira* (SL = 281 mm), (12) *Helicolenus hilgendorfii* (SL = 177 mm), (13) *Sebastes oblongus*, (14) *Sebastes zonatus*, (15) *Chelidonichthys spinosus* (SL = 237 mm), (16) *Acropoma hanedai*, (17) *Trachurus japonicus*, (18) *Pagrus major*, (19) *Sillago japonica* (SL = 211 mm), (20) *Histiopterus typus*, (21) *Scarus forsteni*, (22) *Sphyraena pinguis* (SL = 291 mm), (23) *Rexea prometheoides*, (24) *Scomber japonicus*, (25) *Thunnus orientalis* (SL = 429 mm), (26) *Thunnus tonggol*, (27) *Paralichthys olivaceus*, (28) *Hippoglossoides dubius*, (29) *Macrorhamphosodes uradoi* (SL = 146 mm), (30) *Takifugu pardalis*, (31) *Takifugu snyderi*, (32) *Takifugu stictonotus*. Abbreviations: D, dorsal; V, ventral; R, right; L, left. The directions of the dorsal-ventral axis and the left–right axis in all images are the same as shown in (1) *M. cinereus*. All transverse sections are raw CT scan slices, and the brightness and contrast of all images were adjusted for display. Arrowheads indicate the ridges or trabeculae in lateral sides. Scale bars: 1 mm

(Figure 2[10]) The transverse ridges connected the neural and hemal arches. In addition, circular dimples were at the base of the neural arch.

3.2.7 | Beloniformes

In *Cololabis saira* (Pacific saury), vertebral bodies had a thick and low longitudinal ridge in the middle of the lateral side (Figure 2[11]).

3.2.8 | Perciformes

The vertebral bodies of *Helicolenus hilgendorfii*, *Sebastes oblongus*, *Sebastes zonatus*, *Acropoma hanedai*, *Pagrus major* (Japanese seabream), *Thunnus orientalis* (Pacific bluefin tuna), and *Thunnus tonggol* (Longtail tuna) had one thick plate-like ridge running longitudinally on their mid-lateral sides (Figures 2[12–14, 16, 18, 25, 26]). Also, in all species except *Thunnus orientalis*, circular dimples were on the surface of the vertebral bodies (Figures 2[12–14, 16, 18, 26]). In *Thunnus orientalis*, the surface was smooth (Figure 2[25]).

In *Helicolenus hilgendorfii* and *Sebastes oblongus*, the thick plate-like ridge was formed by a bundle of multiple thin ridges (Figures 2 [12, 13]). In *Thunnus orientalis* and *Thunnus tonggol*, longitudinal grooves were on the surface of the thick ridge (Figures 2[25, 26]).

Some species in Perciformes did not have the thick plate-like ridge in the mid-lateral side of the vertebral body. In *Chelidonichthys spinosus* (Spiny red gurnard), vertebral bodies had the net-like structure formed by a set of thin trabeculae running longitudinally and transversely (Figure 2[15]). Similarly, in *Histiopterus typus* (Sailfin armourhead), the vertebral body had the net-like structure formed by thin sheet-like trabeculae running longitudinally and transversely (Figure 2[20]). In *Sillago japonica* (Silver sillago), a longitudinal thin plate-like ridge was in the middle of the lateral side (Figure 2[19]). In *Rexea prometheoides* (Royal escolar), a longitudinal plate-like ridge connected to the hemal arch was formed (Figure 2[23]). In *Trachurus japonicus* (Japanese jack mackerel), *Scarus forsteni* (Forsten's parrotfish), *Sphyraena pinguis* (Red barracuda), and *Scomber japonicus* (Chub mackerel), no ridge or trabeculae were on the lateral side (Figures 2[17, 21, 22, 24]). The circular dimples were on the surface of their vertebral bodies.

3.2.9 | Pleuronectiformes

In *Paralichthys olivaceus* (Bastard halibut), the vertebral body had three plate-like ridges with multiple longitudinal trabeculae closely attached on the lateral side (Figure 2[27]). Many fine transverse trabeculae were around the plate-like ridges. In *Hippoglossoides dubius* (Flathead flounder), the vertebral body had four longitudinal and over 10 transverse trabeculae that formed a net-like structure. Some circular dimples were on the edge of the longitudinal trabeculae (Figure 2[28]).

3.2.10 | Tetraodontiformes

In *Macrorhamphosodes uradoi*, the vertebral body had almost no ridge (Figure 2[29]). In *Takifugu pardalis*, the vertebral body had one thick longitudinal ridge (Figure 2[30]). In *Takifugu snyderi* and *Takifugu stictonotus*, the net-like structure was formed by multiple longitudinal and transverse trabeculae and was on the lateral side of the vertebral body. Also, one longitudinal thin ridge was on the side of the vertebral body (Figures 2[31, 32]). In all four species, the vertebral arches had the net-like structure formed by thin trabeculae.

In summary, the external shapes of vertebral bodies showed considerable variation among species. Interestingly, shape variation of vertebral bodies among species in the same order was sometimes larger than that among species in different orders. For instance, although *Macrorhamphosodes uradoi*, *Takifugu pardalis*, *Takifugu snyderi*, and *Takifugu stictonotus* belong to the order Tetraodontiformes, their vertebral bodies had different shapes such as no ridge, no trabeculae, thick longitudinal ridge, and the net-like structure, respectively. Conversely, the vertebral bodies of *Zenopsis nebulosa* and *Paralichthys olivaceus* had a similar thick plate-like ridges formed by aggregation of multiple longitudinal trabeculae, despite them belonging to different orders. Some morphological characteristics were commonly observed among the different phylogenetic groups.

3.3 | Transverse section observation

To observe the internal morphological features of the vertebral bodies, we examined transverse sections and found that vertebral bodies with different external shapes shared some internal structures. On the internal side of the vertebral bone, we observed many straight lines radially extending from the center in most of the species (Figure 3). The external end of the lines corresponded to the trabeculae or the longitudinal ridges observed in the lateral view. As they were linear in both the lateral view and in the transverse sections, their shape was a flat sheet-like form. These sheet-like trabeculae were clearly observed in most of the vertebrae with plate-like ridges and net-like trabeculae. The difference in the external shape of the vertebrae was because of the stacking of the sheet-like trabeculae. For example, the net-like structures from the vertebral bodies of Lophiiformes were formed with longitudinal trabeculae arranged at intervals, whereas the thick plate-like ridges of Zeiformes were formed by the stack of longitudinal trabeculae closely attached to each other. Furthermore, the sheet-like trabeculae were also in both neural and hemal arches. To confirm that the characteristics of the sheet-like trabeculae were identical regardless of their region in an individual vertebral body, we measured thickness and angle of the sheet-like trabeculae (Figures 4 and 6; Figure S5). Another structural feature was hollow spaces, which are vacant regions without any bone tissue in the internal part of vertebral bodies. We described the internal structures of the ridges and trabeculae in each species, and then analyzed the characteristics of these sheet-like trabeculae in more detail (Figures 4–7). The characteristics described below are shared among the multiple individuals we examined from the same species.

3.3.1 | Anguilliformes

In *Muraenesox cinereus*, the ridges, which were observed as longitudinal ridges in the lateral view, were composed of dense bone and extended linearly from the center of the vertebral body (Figures 2 [1] and 3[1]). These ridges branched into the fine trabeculae. The ridges observed as transverse ridges in the lateral view were connected to the hemal arches on each lateral side (Figures 2[1] and 3[1]).
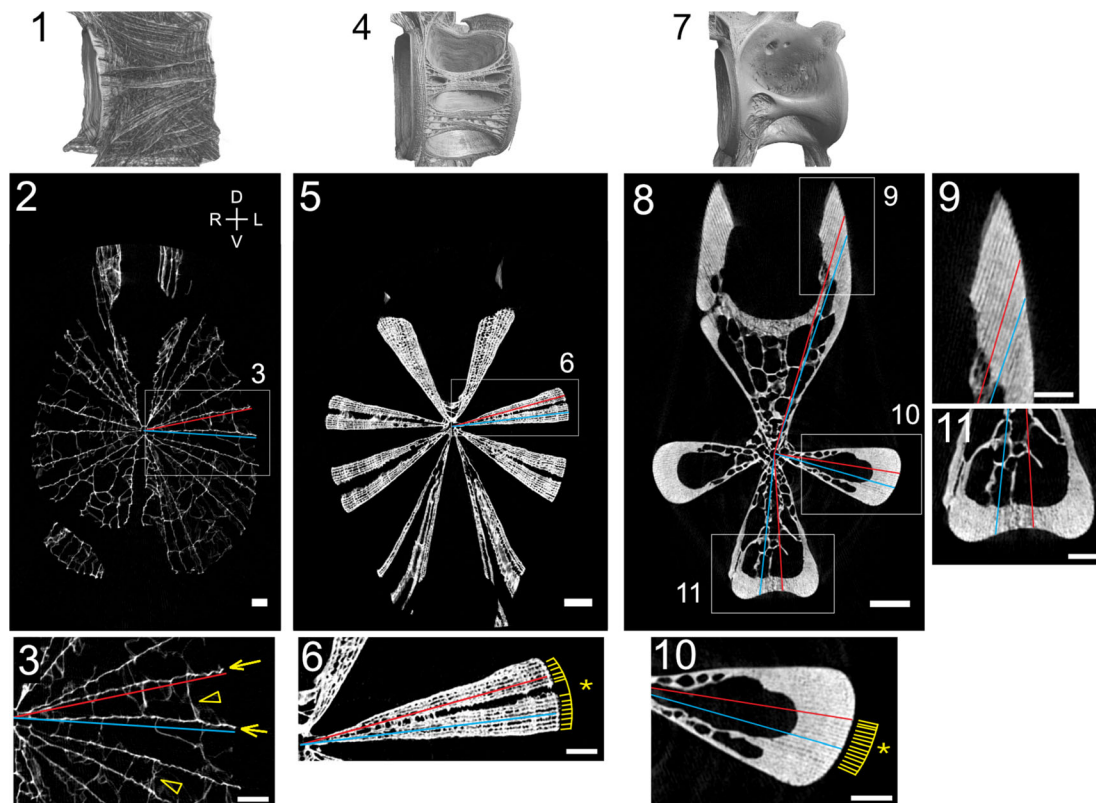
FIGURE 4 Sheet-like trabeculae in different arrangements. (1, 4, 7) Volume-rendered micro-CT scan images showing left lateral views of the vertebral bodies. (2, 5, 8) Transverse sections at the midpoint of the vertebral bodies. Images are of vertebral bodies with the first hemal arch of (1, 2) *Lophius litulon* (SL = 452 mm, centrum length = 10.58 mm), (4, 5) *Zenopsis nebulosa* (SL = 360 mm, centrum length = 7.24 mm), and (7, 8) *Thunnus orientalis* (SL = 429 mm, centrum length = 7.36 mm). (3, 6, and [9, 10, 11]) Magnified images of the areas marked with rectangles in 2, 5, and 8, respectively. Note that each longitudinal trabecula on the lateral side of the vertebral body in *L. litulon* is formed by a longitudinal sheet-like trabecula (yellow arrows) and that the longitudinal plate-like ridge in *Z. nebulosa* and *T. orientalis* is formed by the bundle of sheet-like trabeculae (yellow lines marked by yellow asterisk indicate each sheet-like trabecula). Red and blue straight lines indicate that the direction of the sheet-like trabeculae is exactly radial from the center of the vertebral body both in the lateral ridges and the neural and hemal arches. Yellow arrowheads indicate circumferential trabeculae forming concentric lines in transverse sections. All transverse sections are raw CT scan slices. The brightness and contrast of (2, 3, 5, 6, 8–11) are adjusted for display. Abbreviations: D, dorsal; V, ventral; R, right; L, left. The directions of the dorsal-ventral axis and the left–right axis in all images are the same as shown in (2) *L. litulon*. Scale bars: (2, 3, 5, 8) 1 mm, (6, 9, 10, 11) 500 μm

3.3.2 | Clupeiformes

In *Sardinops melanostictus* and *Konosirus punctatus*, the small ridge composed of dense bone extended from the center of the vertebral body on each lateral side (Figures 3[2] and 3[3]).

3.3.3 | Osmeriformes

In *Plecoglossus altivelis altivelis*, three ridges extended linearly from the center of the vertebral body on each lateral side (Figure 3[4]). These ridges branched and fused into five ridges on the distal edge of the right side and into six ridges on the left side.

3.3.4 | Lophiiformes

In *Lophiomus setigerus*, *Lophius litulon*, and *Chaunax abei*, multiple straight lines indicating sheet-like trabeculae extended from the center of the vertebrae (Figures 3[5–7]). The sheet-like trabeculae were

distributed at almost equal intervals in the vertebral body of *Lophius litulon* (Figure 3[6]), whereas they were gathered in the middle on the lateral side in *Lophiomus setigerus* and *Chaunax abei* (Figures 3[5] and 3[7]). In the three species, the sheet-like trabeculae were also in the neural and hemal arches.

3.3.5 | Zeiformes

In *Zenopsis nebulosa* and *Zeus faber*, the straight lines of sheet-like trabeculae extending linearly in a radial direction were closely attached to each other, forming two thick plate-like ridges on each lateral side (Figures 3[8, 9]). The sheet-like trabeculae were also in the neural and hemal arches. All sheet-like trabeculae extended directly from the center of the vertebral body in *Zenopsis nebulosa* (Figure 3[8]), whereas sheet-like trabeculae were present only at the distal edge of the ridges and hollow spaces formed in the sclerotomal bone (Figure 3[9]).
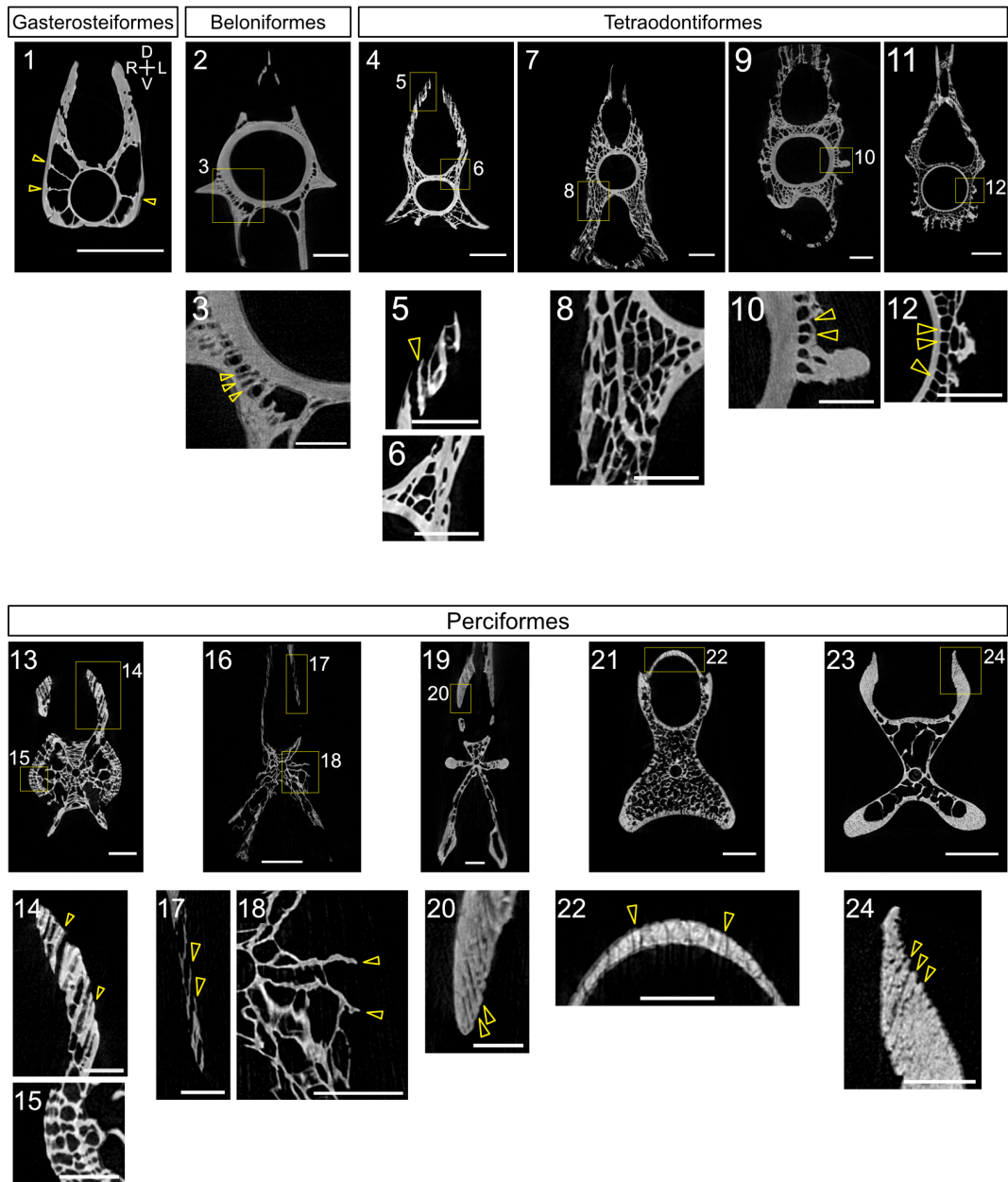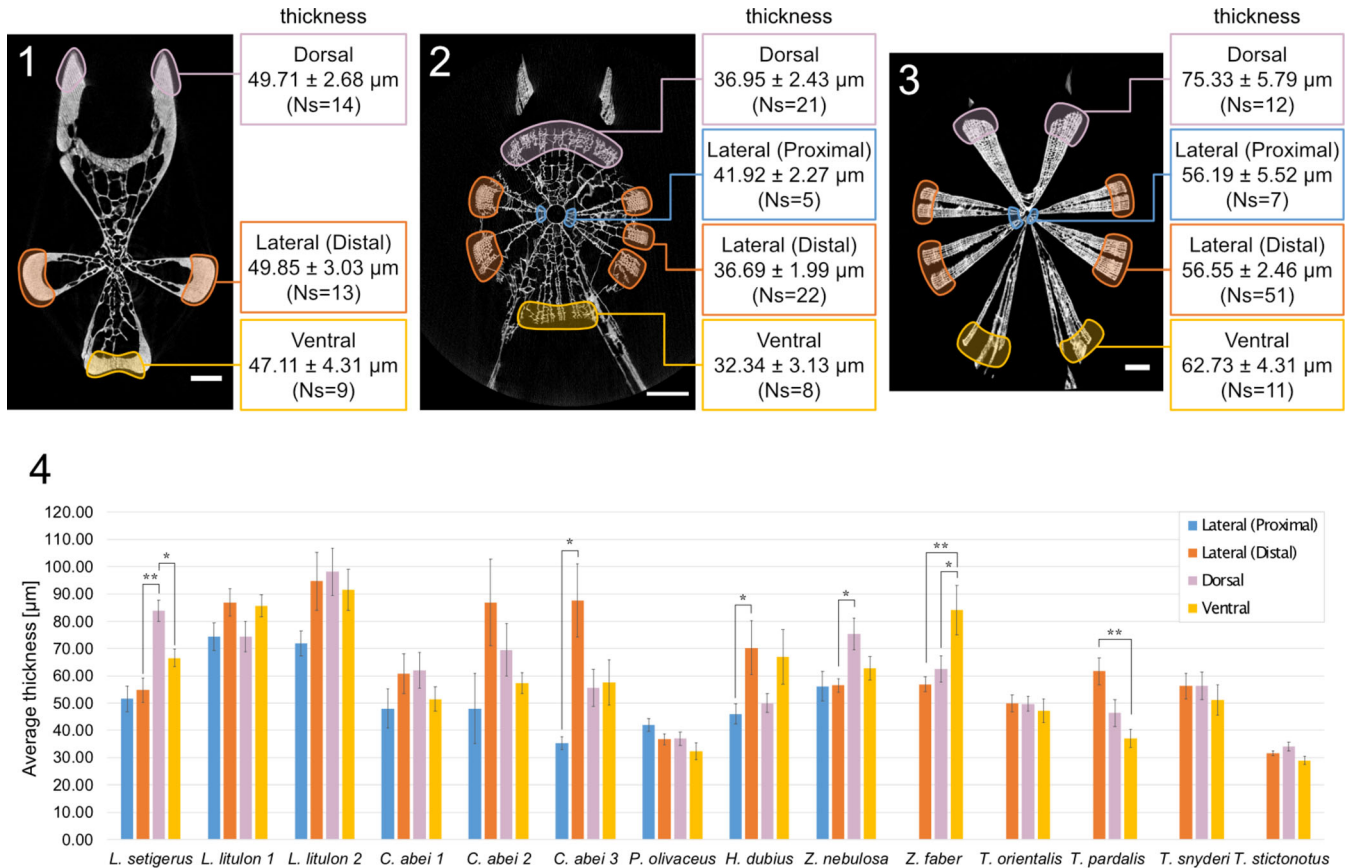
FIGURE 5 Transverse sections of vertebral bodies with the first hemal arch showing sheet-like trabeculae. All transverse sections are raw CT scan slices. (1, 2, 4, 7, 9, 11) Transverse sections of the vertebral bodies of (1) *Macroramphosus sagifue* (SL = 90 mm), (2) *Cololabis saira* (SL = 281 mm), (4) *Macrorhamphosodes uradoi* (SL = 146 mm), (7) *Takifugu pardalis*, (9) *Takifugu snyderi*, and (11) *Takifugu stictonotus*. These images are of the anterior (1, 2, 4, 7, 9) and posterior (11) sections of the same vertebrae presented in Figure 3. (13, 16, 19, 21, 23) Transverse sections at the midpoint of the vertebral bodies of (13) *Chelidonichthys spinosus* (SL = 237 mm), (16) *Histiopterus typus*, (19) *Sebastes zonatus*, (21) *Scomber japonicus*, (23) *Rexea prometheoides*. All images of (1, 2, 4, 7, 9, 11, 13, 16, 19, 21, 23) are from the vertebra with the first hemal arch of each specimen. (3, 5, 6, 8, 10, 12, 14, 15, 17, 18, 20, 22, 24) Magnified images of the areas marked with yellow rectangles in (2, 4, 7, 9, 11, 13, 16, 19, 21, 23). Each image shows the straight radial lines indicating the sheet-like trabeculae (yellow arrowheads). The brightness and contrast of all images are adjusted for display. Abbreviations: D, dorsal; V: ventral; R: right; L: left. The directions of the dorsal-ventral axis and the left–right axis in all images are the same as shown in (1) *M. sagifue*. Scale bars: (1, 2, 4, 7, 9, 11, 13, 16, 19, 21, 23) 1 mm, (3, 5, 6, 8, 10, 12, 14, 15, 18, 20, 22) 500 μm, (17, 24) 300 μm

3.3.6 | Gasterosteiformes

In *Macroramphosus sagifue*, one thin ridge composed of dense bone extended from the center of the vertebral body on each lateral side (Figure 3[10]).

3.3.7 | Beloniformes

In *Cololabis saira*, one thick ridge made of dense bone extended from the center of the vertebral body on each lateral side (Figure 3[11]).

FIGURE 6 Measurements of the sheet-like trabeculae thickness. (1–3) Transverse sections at the midpoint of the vertebral bodies with the first hemal arch, showing the thickness of the sheet-like trabeculae in the dorsal and ventral regions of the vertebral arches and the proximal or distal regions of the lateral sides. The colored ellipse surrounding the sheet-like trabeculae indicates the location where thickness was measured. The images show that the difference of the sheet-like trabeculae thickness is less than 1.3-fold in each specimen. (1) *Thunnus orientalis* (SL = 429 mm, centrum length = 7.36 mm), (2) *Paralichthys olivaceus* (SL = 218 mm, centrum length = 4.14 mm), and (3) *Zenopsis nebulosa* (SL = 360 mm, centrum length = 7.24 mm). All transverse sections are raw CT scan slices. The brightness and contrast of (1–3) are adjusted for display. Scale bars: (1–3) 1 mm. (4) Thickness of sheet-like trabeculae of vertebra with the first hemal arch in 14 individuals from 11 species. *$p < .05$, **$p < .01$. Welch's t-test was performed for the comparison between lateral proximal and lateral distal regions and the Tukey HSD test was performed for the comparison of dorsal, ventral, and lateral distal regions. Error bars indicate the standard error. The value of average thickness and standard error of each specimen is described in Table 2

3.3.8 | Perciformes

In *Helicolenus hilgendorfii*, *Sebastes oblongus*, *Sebastes zonatus*, and *Pagrus major*, one thick ridge of dense bone extended from the center of the vertebral body on each lateral side. Many hollow spaces were in the ridge and in the neural and hemal arches (Figures 3[12–14, 18]). Similarly, in *Thunnus orientalis* and *Thunnus tonggol*, one thick ridge on each lateral side was made of dense bone and the internal part was almost hollow (Figures 3[25, 26]). In *Acropoma hanedai* and *Sillago japonica*, one thin ridge of dense bone extended from the center of the vertebral body on each lateral side. There were no hollow spaces on the internal part of the ridge (Figures 3[16, 19]). In *Histiopterus typus*, two thin sheet-like trabeculae extended from the center of the vertebral body on each lateral side. Sheet-like trabeculae were also in the neural and hemal arches (Figure 3[20]). In *Chelidonichthys spinosus*, sheet-like trabeculae extended linearly in the radial direction on the distal edge of the lateral sclerotomal bone and the neural arch.

Contrarily, in the center, trabeculae were not sheet-like shaped and had hollow spaces (Figure 3[15]). In *Trachurus japonicus*, *Rexea prometheoides*, and *Scomber japonicus*, the external part of the sclerotomal bone was covered with dense bone, and the internal part had hollow spaces (Figures 3[17, 23, 24]). In *Scarus forsteni* and *Sphyraena pinguis*, the sclerotomal bone was made of dense bone, and hollow spaces were present in the neural and hemal arches. The cylindrical form in the center collapsed to form radial fissures, but the shape of the internal part of the sclerotomal bone was an amphicoelous hourglass shape as in other species (Figures 3[21, 22]; Figures S4. 10′ and S4. 11′).

3.3.9 | Pleuronectiformes

In *Paralichthys olivaceus*, two or three ridges extended radially from the center of the vertebral body on each side, and more sheet-like trabeculae were at the distal edge than near the center of the vertebral
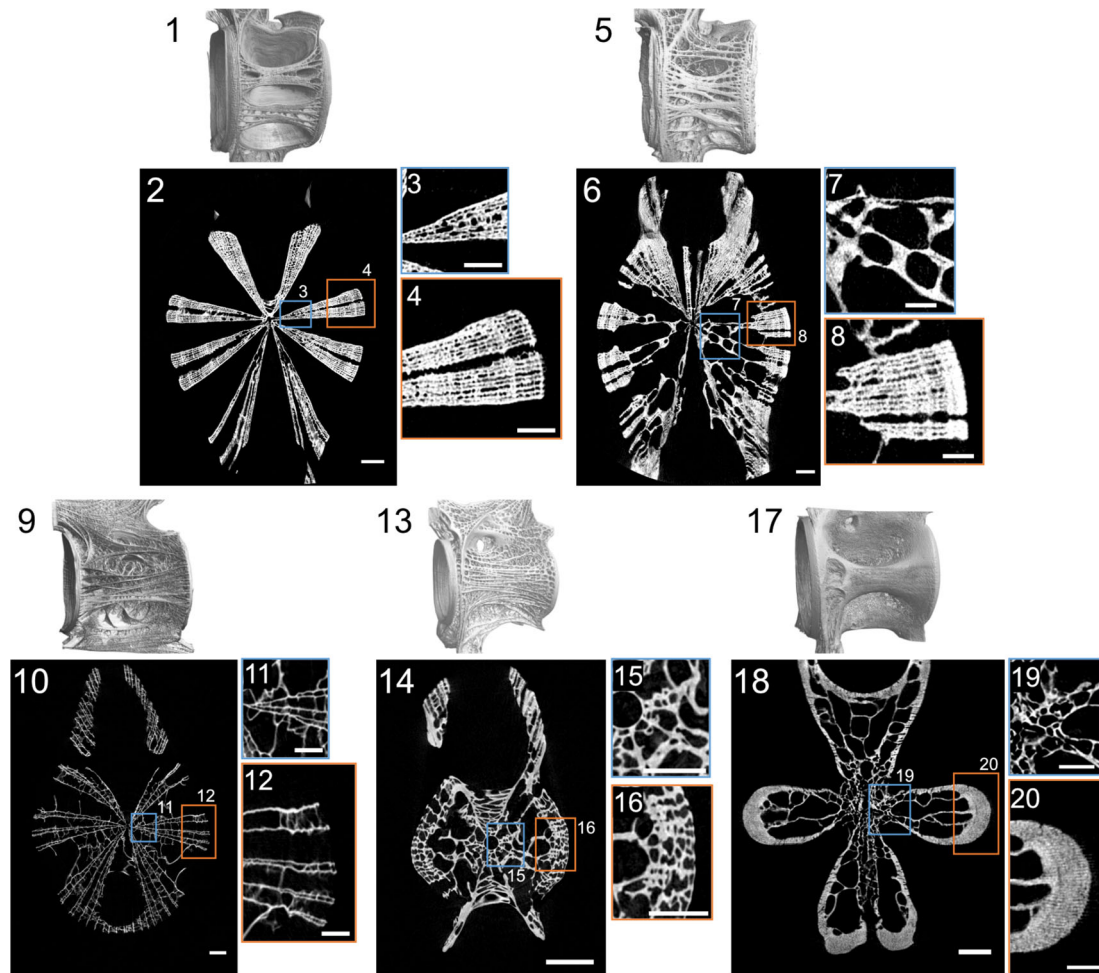
FIGURE 7 Comparison of the presence and absence of internal hollow spaces. (1, 5, 9, 13, 17) Volume-rendered micro-CT images showing the left lateral view of vertebral bodies. (2, 6, 10, 14, 18) Transverse sections at the midpoint of vertebral bodies. Each image is of a vertebral body with the first hemal arch: (1, 2) *Zenopsis nebulosa* (SL = 360 mm, centrum length = 7.24 mm), (5, 6) *Zeus faber* (SL = 359 mm, centrum length = 8.75 mm), (9, 10) *Lophiomus setigerus* (SL = 285 mm, centrum length = 10.73 mm), (13, 14) *Chelidonichthys spinosus* (SL = 237 mm, centrum length = 4.76 mm), and (17, 18) *Thunnus tonggol* (TL = 550 mm, centrum length = 8.49 mm). (3, 4, 7, 8, 11, 12, 15, 16, 19, 20) Magnified images of the areas marked with rectangles in (2, 6, 10, 14, 18). Note that the sheet-like trabeculae can be observed both around the center of the vertebral bodies and at the end of the lateral structure in *Z. nebulosa* and *L. setigerus*; but the sheet-like trabeculae exist only at the end and cannot be observed around the center in *Z. faber*, *C. spinosus*, and *T. tonggol*. All transverse sections are raw CT scan slices. The brightness and contrast of of (2, 6, 10, 14, 18) are adjusted for display. Scale bars: (2, 6, 10, 14, 18) 1 mm, (3, 4, 7, 8, 11, 12, 15, 16, 19, 20) 500 μm

body (Figure 3[27]). The sheet-like trabeculae also extended dorsally and ventrally in the sclerotomal bone. In *Hippoglossoides dubius*, four sheet-like trabeculae extended radially from the center of the vertebral body on each lateral side (Figure 3[28]).

3.3.10 | Tetraodontiformes

In *Macrorhamphosodes uradoi*, the external part of the sclerotomal bone was covered with dense bone and no ridges or trabeculae were on each side (Figure 3[29]). In *Takifugu pardalis*, one thick ridge made of dense bone extended radially from the center of the vertebral body on each side (Figure 3[30]). In *Takifugu snyderi*, one thin ridge made of dense bone and multiple thin trabeculae

extended radially from the center of the vertebral body on each side (Figure 3[31]). In *Takifugu stictonotus*, multiple thin trabeculae extended radially from the center of the vertebral body on each side (Figure 3[32]. See also Figure 5[11]). In all four species, fine trabeculae were present in the neural and hemal arches (Figures 3[29–32]).

3.4 | Sheet-like trabeculae

We further detailed the morphological features of the sheet-like trabeculae by examining the species *Lophius litulon*, *Zenopsis nebulosa*, and *Thunnus orientalis*. These species exhibited significantly different shapes of sclerotomal bones, and the sheet-like trabeculae were more

evident than in other species with similar external shapes. Therefore, the structural characteristics of their sheet-like trabeculae were clearly observed. The 3D configuration (shape, angle, and arrangement) of the sheet-like trabeculae are in Movies S1, S2, and S3. Concerning the vertebral body of *Lophius litulon*, characteristics of the trabeculae are more visible because they are sparsely distributed. In transverse view, longitudinal trabeculae are straight lines with uniform width extending radially from the center. In 3D, these longitudinal trabeculae are the flat sheet-like structures radially and sparsely distributed (Movie S1, Figures 4[1–3]). They are also connected by the thin circumferential trabeculae that form concentric lines (indicated by yellow arrowheads in Figures 4[2, 3]). The radial lines and circumferential lines indicating the longitudinal and transverse trabeculae were also in *Zenopsis nebulosa* (Figures 4[4–6]). Although the characteristics (flatness, angle) of each trabecula are very similar, they were densely attached to each other to form the thick plate-like ridges (Figure 4[6] and Movie S2). The transverse and sagittal sections of *Thunnus orientalis* showing the thick plate-like ridge also indicated that they are composed of similar trabeculae with the flat sheet-like shape (Figures 4[7, 8, 10] and Movie S3). The longitudinal grooves on the surface of the ridge correspond to the tips of each sheet-like trabecula (Figure 2[26]). Interestingly, in all specimens of *Lophius litulon*, *Zenopsis nebulosa*, and *Thunnus orientalis*, the sheet-like trabeculae were observed not only in the lateral side of the vertebral body but also in the neural and hemal arches. The angle of the sheet-like trabeculae in the neural and hemal arches was exactly radial from the center of the vertebral body, even in the regions where the sheet-like trabeculae were not directly connected to the center (Figures 4[3, 6, 9–11]). In the transverse section of midpoint of the vertebral body (Figure 3), the sheet-like trabeculae were not well visible in many other species. However, they can be observed in the sections at different positions along the cranio-caudal axis in *Macroramphosus sagifue*, *Cololabis saira*, *Macrorhamphosodes uradoi*, *Takifugu pardalis*, and *Takifugu snyderi* (Figures 5[1–12]). The sheet-like trabeculae in arches were also present in other species such as *Chelidonichthys spinosus*, *Histiopterus typus*, *Sebastes zonatus*, *Scomber japonicus*, and *Rexea prometheoides* (Figures 5[13–24]). In total, the sheet-like trabeculae were detected in 20 of the 32 examined species. Hence, it was expected that the sheet-like trabeculae were a shared basic structural unit among the species in Teleostei. Another important characteristic of the sheet-like trabeculae as a structural unit was its thickness. We measured the thickness of sheet-like trabeculae from different regions of the vertebral body and of the neural and hemal arches in 14 individuals of 11 species, in which the trabeculae could be clearly observed (Table 2, the measurement method is illustrated in Figure S3). The graph in Figure 6 shows these results. The thickness of the sheet-like trabeculae ranged from 30–100 μm (Figure 6[4]). However, within the same individual, the thickness was roughly the same irrespective of the position of the trabecula in the vertebral body. For example, in *Lophius litulon*, *Zenopsis nebulosa*, *Thunnus orientalis*, *Paralichthys olivaceus*, *Takifugu snyderi*, and *Takifugu stictonotus* the difference in the thickness between the vertebral body trabeculae and the neural and hemal arch trabeculae was small (less than 1.3-fold; Figures 6 and Figure S5).

In *Lophiomus setigerus*, *Chaunax abei*, *Zeus faber*, *Takifugu pardalis*, and *Hippoglossoides dubius* the difference was relatively larger, but remained within the range of 1.7-fold. A more impressive result was the small difference of the trabecular thickness between the proximal part and the distal edge of the vertebral body. In *Zenopsis nebulosa*, although the lateral ridge was more than seven times thicker in the distal part than in the proximal one, the thickness of each trabecula was almost the same (Figure 6 and Table 2). Instead, the number of trabeculae increased. This was also observed in *Lophiomus setigerus*, *Lophius litulon*, and *Paralichthys olivaceus* (Figure S5; Table 2).

3.5 | Internal hollow spaces

Another structural feature of the vertebral bodies is the hollow spaces on its proximal region. Even in species with similar external shapes of sheet-like trabeculae, their internal structures differ by the presence or absence of the hollow spaces (Figure 7). For instance, *Zenopsis nebulosa* and *Zeus faber*, which are closely related members of the family Zeidae (based on genetic data; Grande, Borden, Wilson, & Scarpitta, 2018), exhibit similar external shapes of vertebral bodies; however, the sheet-like trabeculae of *Zenopsis nebulosa* continuously extended from the center to the surface of the vertebral body, whereas in *Zeus faber* the sheet-like trabeculae were absent in the center of the vertebral body, existing only on the surface region (Figures 7[1–8]).

In *Lophiomus setigerus*, in Lophiiformes, and *Chelidonichthys spinosus*, in Perciformes, both with similar net-like structures, sheet-like trabeculae were intact in *Lophiomus setigerus*, whereas the trabeculae in the internal part were replaced by the hollow spaces in *Chelidonichthys spinosus* (Figures 7[9–16]). These hollow spaces were widely observed in the vertebral bodies of *Helicolenus hilgendorfii*, *Sebastes oblongus*, *Sebastes zonatus*, *Trachurus japonicus*, *Pagrus major*, *Scarus forsteni*, *Sphyraena pinguis*, *Rexea prometheoides*, *Scomber japonicus*, *Thunnus orientalis*, and *Thunnus tonggol* in Perciformes (Figures 3[12, 13, 14, 17, 18, 21–26]). The angle of the radial sheet-like trabeculae at the distal regions was not affected by the presence or absence of the hollow spaces (Figures 7[6–8, 14–16, 18–20]). Therefore, it seems that the hollow spaces appeared after the sheet-like trabeculae, and probably through an independent mechanism.

4 | DISCUSSION

In this study, we observed the fine 3D-structure of vertebral bodies of 32 species from 10 orders of teleost fishes using micro-CT scans, and found two common structural units: the sheet-like trabeculae and the internal hollow spaces. Twenty-six examined species had either one or both feature, that is, sheet-like trabeculae and internal hollow spaces, these two structural features were hypothesized to be shared among teleost species.

TABLE 2 Thickness of the sheet-like trabeculae of 14 individuals from 11 species based on the measurements of the vertebrae with the first hemal arch

Species	Sample no.	Standard length (mm)	Lateral (proximal)			Lateral (distal)			Dorsal			Ventral		
			Ns	Average thickness (µm)	Standard error (µm)	Ns	Average thickness (µm)	Standard error (µm)	Ns	Average thickness (µm)	Standard error (µm)	Ns	Average thickness (µm)	Standard error (µm)
Lophiomus setigerus	1	285	2	51.59	4.69	18	54.72	4.44	30	83.80	3.89	20	66.60	3.11
Lophius litulon	1	452	4	74.46	5.07	10	86.87	4.90	10	74.46	5.55	10	85.63	3.90
	2	623	5	71.98	4.64	7	94.61	10.61	18	98.11	8.70	11	91.56	7.51
Chaunax abei	1	188	3	47.95	7.21	8	60.76	7.37	4	62.00	6.56	8	51.46	4.39
	2	209	3	48.00	12.93	6	86.90	15.79	7	69.52	9.63	9	57.38	3.89
	3	178	2	35.18	2.35	6	87.56	13.36	6	55.51	6.79	7	57.63	8.30
Paralichthys olivaceus	1	218	5	41.92	2.27	22	36.69	1.99	21	36.95	2.43	8	32.34	3.13
Hippoglossoides dubius	1	150**	7	45.99	3.71	13	70.22	9.93	6	49.98	3.54	5	67.03	10.00
Zenopsis nebulosa	1	360	7	56.19	5.52	51	56.55	2.46	12	75.33	5.79	11	62.73	4.31
Zeus faber	1	359	ND	ND	ND	35	56.91	2.71	7	62.47	4.81	4	84.10	9.08
Thunnus orientalis	1	429	ND	ND	ND	13	49.85	3.03	14	49.71	2.68	9	47.11	4.31
Takifugu pardalis	1	170*	ND	ND	ND	9	61.74	4.99	8	46.31	4.86	8	36.93	3.33
Takifugu snyderi	1	210*	ND	ND	ND	12	56.21	4.62	14	56.33	5.06	10	51.09	5.63
Takifugu stictonotus	1	93**	ND	ND	ND	22	31.56	0.95	13	33.96	1.57	6	28.93	1.52

Notes. In Standard length, * indicates total length (TL), and ** indicates the sum of the lengths of all vertebrae, except the urostyle. Ns indicates the number of sheet-like trabeculae measured. ND (No Data) indicates that the sheet-like trabecula was not detected on the internal part of the lateral structure in Z. faber and T. orientalis. Also, it indicates that the proximal and distal regions of the sheet-like trabeculae could not be distinguished in T. pardalis, T. snyderi, and T. stictonotus, as the lines that are used to identify the sheet-like trabeculae were too short. Lateral (proximal or distal), dorsal, and ventral regions in which we obtained the brightness plots of each specimen are illustrated in Figure S5.
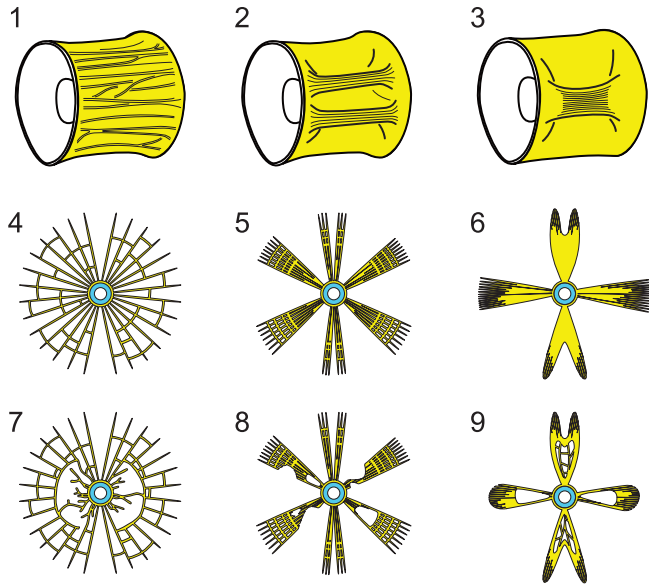
FIGURE 8 Schematic illustration of the combination of the sheet-like trabeculae and the internal hollow spaces for the formation of the different shapes of the sclerotomal bone. (1–3) Left lateral view of vertebral bodies with (1) the net-like structure, (2) two thick plate-like ridges, (3) one thick plate-like ridge. (4–6) Transverse sections at midpoint of the vertebral body (1–3), respectively. The images (4–6) show the different arrangements of the sheet-like trabeculae: the sheet-like trabeculae are arranged sparsely in (4) and the multiple sheet-like trabeculae are closely attached to form the thick plate-like ridges in (5) and (6). (7–9) Transverse sections at midpoint of the vertebral body (1–3). The arrangements of the sheet-like trabeculae are the same in (4–6), respectively, but the images of (7–9) show the internal hollow spaces

4.1 | Combination of sheet-like trabeculae and internal hollow spaces

The variations in the 3D shape of the vertebrae can be generated by different arrangements of two common elements (Figure 8). The first element is the sheet-like trabeculae, which have flat shape and uniform thickness and extend radially from the center of the vertebrae. When the sheet-like trabeculae were spaced apart (without stacking), they formed a net-like structure; this was observed in *Lophiomus setigerus*, *Lophius litulon*, *Chaunax abei*, *Histiopterus typus*, *Hippoglossoides dubius*, *Macrorhamphosodes uradoi*, *Takifugu pardalis*, *Takifugu snyderi*, and *Takifugu stictonotus* (Figures 8[1, 4]). Also, densely stacked trabeculae form a plate-like ridge (Figures 8[2, 3, 5, 6]). Different stacking, may create different bone morphologies. When the sheet-like trabeculae were stacked in one place, they formed a single thick ridge, as in *Cololabis saira*. When gathering in two or three places, they formed ridges resembling the outlines of *Zenopsis nebulosa* or *Paralichthys olivaceus* (Figures 8[5, 6]). Therefore, the external shape of the vertebrae was mostly determined by how the sheet-like trabeculae were stacked.

The second element was the hollow spaces that occur near the center of the sclerotomal bone. In *Chelidonichthys spinosus*, *Zeus faber*, *Sebastes zonatus*, *Thunnus tonggol*, and *Thunnus orientalis*, hollow spaces were found irrespective to the different arrangement of the

sheet-like trabeculae (Figures 8[7–9]). Even between closely related species, there was a difference in the presence and absence of the hollow spaces. For example, among species with one thick ridge, the vertebrae of *Sardinops melanostictus*, *Konosirus punctatus*, *Acropoma hanedai*, and *Sillago japonica* did not have internal hollow spaces (Figure 8[6]), whereas those of *Helicolenus hilgendorfii*, *Sebastes oblongus*, and *Pagrus major* had internal hollow spaces (Figure 8[9]). Therefore, the presence or absence of the hollow spaces is another parameter that categorizes the shape of the vertebrae.

These data help us understand the diversity of sclerotomal bone shapes among teleosts in a unified context. Some species shown in this paper were not separated in the proposed categories as the sheet-like trabeculae were not identified. However, this could be because of the limit of detection of the micro-CT scans. The use of higher-resolution CT scans (e.g., synchrotron X-ray CT scans) or of younger specimens may allow the detection of sheet-like trabeculae in these species and, consequently, their inclusion in the proposed categories.

4.2 | Formation of sheet-like trabeculae

Nordvik et al. (2005) reported that, in the Atlantic salmon, the lateral sides of each vertebral body have trabeculae extending radially and branching from the center. In addition, they observed that the tips of each trabeculae are covered with densely assembled osteoblasts. Based on these facts, they hypothesized that the vertebral body grows outward by adding bone selectively to the end of the trabeculae. Our results showed that trabecular structures with similar properties are common structural units in the fish vertebrae. Therefore, the prediction of Nordvik et al. (2005) is likely to be applicable to fish in general. However, the presence of osteoblasts at the tip is insufficient to explain the precise radial angle that the sheet-like trabeculae maintain even in the region far from the center of the vertebral body. It is also insufficient to explain how the sheet-like trabeculae correctly keep the same thickness. We hope future studies will solve this problem.

4.3 | Formation of internal hollow spaces

In the comparative studies in the broader range of the phylogenetic groups, we discovered that some species of fish have internal hollow spaces which have not been identified in previous studies. So far, the current models of morphogenesis of the sclerotomal bone do not take into account bone remodeling (Nordvik et al., 2005), as they did not identify the presence of osteoclasts in the vertebral body of teleost fish (Witten & Villwock, 1997) or they identified only a few degraded osteocytes (Cao et al., 2011). However, recent reports by Atkins et al. (2014) reject the suggestions of these former studies; they detected the presence of secondary osteons in rostral bones of billfishes, which indicates bone remodeling. Moreover, they showed an example of bone remodeling occurring as a response to the external loading of mechanical stress (Atkins, Milgram, Weiner, & Shahar, 2015). The presence of the internal hollow spaces as documented here suggests

that the bone absorption occurred at the proximal region of the vertebrae, thus supporting the latter possibility. Which type of cells form the internal hollow spaces is a question that remains to be elucidated and, for this, more histological studies on the developmental stages from juvenile to adult are needed.

4.4 | Component of the vertebral body and vertebral arch

In Teleostei, the vertebrae of extant species are composed of four major components: chordacentrum, autocentrum, the cartilaginous arcualia and arcocentrum (Arratia et al., 2001). Currently, there are multiple opinions about which components form the vertebral arches. Arratia et al. (2001) suggested that the autocentrum forms the internal amphicoelous hourglass shape and the external lateral structure, while the arcocentrum only forms the vertebral arches. However, Nordvik et al. (2005) suggested that the arcocentrum covers the hourglass-shaped autocentrum to form the external lateral structure of the vertebral body as well as the vertebral arches. A comparative study among other teleost species is required to clarify this discrepancy. In this article, we show that both the vertebral body and vertebral arches were formed of the sheet-like trabeculae with identical characteristics in 20 teleost species. Therefore, our data supports the hypothesis of Nordvik et al. (2005), that the vertebral body and arches are constituted of the same components.

AUTHORS CONTRIBUTIONS

M. Sakashita and S. Kondo designed the study strategy. M. Sakashita performed the collection of the fish, preparation of the skeletal specimens, examination of the vertebrae with micro-CT scans. M. Sato performed the collection of the fish and advised M. Sakashita for the preparation of the skeletal specimens. M. Sakashita wrote the manuscript and all authors commented on the manuscript.

CONFLICT OF INTEREST

The authors have no conflicts of interest to disclose.

ORCID

Misaki Sakashita https://orcid.org/0000-0002-7076-655X
Mao Sato https://orcid.org/0000-0002-8111-7694

REFERENCES

Arratia, G. (1991). Caudal skeleton of Jurassic teleosts; a phylogenetic analysis. In M.-M. Chang, H. Liu, & G. Zhang (Eds.), *Early vertebrates and related problems in evolutionary biology* (pp. 249–282). Beijing: Science Press.

Arratia, G., Schultze, H.-P., & Casciotta, J. (2001). Vertebral column and associated elements in dipnoans and comparison with other fishes: Development of homology. *Journal of Morphology*, 250, 101–172.

Atkins, A., Dean, M. N., Habegger, M. L., Motta, P. J., Ofer, L., Repp, F., … Shahar, R. (2014). Remodeling in bone without osteocytes: Billfish challenge bone structure-function paradigms. *Proceedings of the National Academy of Sciences*, 111, 16047–16052. https://doi.org/10.1073/pnas.1412372111

Atkins, A., Milgram, J., Weiner, S., & Shahar, R. (2015). The response of anosteocytic bone to controlled loading. *Journal of Experimental Biology*, 218, 3559–3569. https://doi.org/10.1242/jeb.124073

Bensimon-Brito, A., Cardeira, J., Cancela, M. L., Huysseune, A., & Witten, P. E. (2012). Distinct patterns of notochord mineralization in zebrafish coincide with the localization of Osteocalcin isoform 1 during early vertebral centra formation. *BMC Developmental Biology*, 12, 28.

Betancur-R, R., Broughton, R. E., Wiley, E. O., Carpenter, K., López, J. A., Li, C., … Ortí, G. (2013). The tree of life and a new classification of bony fishes. *PLOS Currents Tree of Life*, 1, 1–45. https://doi.org/10.1371/currents.tol.53ba26640df0ccaee75bb165c8c26288

Cao, L., Moriishi, T., Miyazaki, T., Iimura, T., Hamagaki, M., Nakane, A., … Yamaguchi, A. (2011). Comparative morphology of the osteocyte lacunocanalicular system in various vertebrates. *Journal of Bone and Mineral Metabolism*, 29, 662–670. https://doi.org/10.1007/s00774-011-0268-6

Eastman, J. T., Witmer, L. M., Ridgely, R. C., & Kuhn, K. L. (2014). Divergence in skeletal mass and bone morphology in Antarctic notothenioid fishes. *Journal of Morphology*, 275(8), 841–861. https://doi.org/10.1002/jmor.20258

Fleming, A., Keynes, R., & Tannahill, D. (2004). A central role for the notochord in vertebral patterning. *Development*, 131, 873–880.

Fleming, A., Kishida, M. G., Kimmel, C. B., & Keynes, R. J. (2015). Building the backbone: The development and evolution of vertebral patterning. *Development*, 142, 1733–1744. https://doi.org/10.1242/dev.118950

Grande, T. C., Borden, W. C., Wilson, M. V. H., & Scarpitta, L. (2018). Phylogenetic relationships among fishes in the order Zeiformes based on molecular and morphological data. *Copeia*, 106(1), 20–48. https://doi.org/10.1643/CG-17-594

Grotmol, S., Kryvi, H., Nordvik, K., & Totland, G. K. (2003). Notochord segmentation may lay down the pathway for the development of the vertebral bodies in the Atlantic salmon. *Anatomy and Embryology*, 207, 263–272.

Grotmol, S., Nordvik, K., Kryvi, H., & Totland, G. K. (2005). A segmental pattern of alkaline phosphatase activity within the notochord coincides with the initial formation of the vertebral bodies. *Journal of Anatomy*, 206, 427–436.

Inohaya, K., Takano, Y., & Kudo, A. (2007). The teleost intervertebral region acts as a growth center of the centrum: in vivo visualization of osteoblasts and their progenitors in transgenic fish. *Developmental Dynamics*, 236, 3031–3046.

Kendall, A. W., Jr., Ahlstrom, E. H., & Moser, H. G. (1984). Early life history stages of fishes and their characters. In H. G. Moser, W. J. Richards, D. M. Cohen, M. P. Fahay, A. W. Kendall, & S. L. Richardson (Eds.), *Ontogeny and systematics of fishes, American society of ichthyologists and herpetologists special publication 1* (pp. 11–22). Lawrence: Allen Press.

Laerm, J. (1976). The development, function, and design of amphicoelous vertebrae in teleost fishes. *Zoological Journal of the Linnean Society*, 58, 237–254.

Masuda, H., Amaoka, K., Araga, C., Uyeno, T., & Yoshino, T. (1984). *The fishes of the Japanese archipelago*. Kanagawa: Tokai University Press.

Nakabo, T. (2013). *Fishes of Japan with pictorial keys to the species* (3rd ed.). Kanagawa: Tokai University Press.

Near, T. J., Eytan, R. I., Dornburg, A., Kuhn, K. L., Moore, J. A., Davis, M. P., ... Smith, W. L. (2012). Resolution of ray-finned fish phylogeny and timing of diversification. *Proceedings of the National Academy of Sciences*, *109*, 13698–13703.

Nelson, J. S., Grande, T. C., & Wilson, M. V. H. (2016). *Fishes of the world* (5th ed.). New Jersey: Wiley.

Nordvik, K., Kryvi, H., Totland, G. K., & Grotmol, S. (2005). The salmon vertebral body develops through mineralization of two preformed tissues that are encompassed by two layers of bone. *Journal of Anatomy*, *206*, 103–114.

Willems, B., Büttner, A., Huysseune, A., Renn, J., Witten, P. E., & Winkler, C. (2012). Conditional ablation of osteoblasts in medaka. *Developmental Biology*, *364*, 128–137.

Witten, P. E., & Villwock, W. (1997). Growth requires bone resorption at particular skeletal elements in a teleost fish with acellular bone (*Oreochromis niloticus*, Teleostei: Cichlidae*). Journal of Applied Ichthyology*, *13*, 149–158.

Wopat, S., Bagwell, J., Sumigray, K. D., Dickson, A. L., Huitema, L. F. A., Poss, K. D., ... Bagnat, M. (2018). Spine patterning is guided by segmentation of the notochord sheath. *Cell Reports*, *22*(8), 2026–2038. https://doi.org/10.1016/j.celrep.2018.01.084

SUPPORTING INFORMATION

Additional supporting information may be found online in the Supporting Information section at the end of this article.